ANALYZING DIFFERENCES IN COLOR VARIATION SENSITIVITY BETWEEN EXPERTS AND NOVICES TO FIND A DIFFERENTIATING PROCESS IN PIGMENTED SKIN LESION DIAGNOSIS

by

YU-CHIN CHAI

Presented to the Faculty of the Graduate School of

The University of Texas at Arlington in Partial Fulfillment

of the Requirements

for the Degree of

MASTER OF SCIENCE IN COMPUTER SCIENCE AND ENGINEERING

THE UNIVERSITY OF TEXAS AT ARLINGTON

May 2007

DEDICATION

To mom

ACKNOWLEDGMENTS

I would like to express my deep gratitude to Dr. Manfred Huber, my supervising professor, for his invaluable advice, encouragement and guidance through the course of this project. I would like also to express my deep gratitude to Mr. David Levine and Dr. Lynn Peterson for serving on my committee. Moreover, this project may not be possible without Dr. Alp Aslandogan, Dr. Paul Bergstresser and Southwestern Medical Center dermatologists' intellectual inputs and helpful feedbacks. My deep thanks would like to go to participants who volunteered to this project. My appreciations would like to go to Dr. Bart Farell, my mentor in my post-doctoral fellowship, for his understanding and insightful advices in biomedical engineering and vision science. Further, I would like to thank to Dr. Ramesh Yeraballi and Mr. Mike O'Dell for the kindness of the guidance. Finally, I would like to give special thanks to B who makes me realize this project does matter to people.

December 18, 2006

ABSTRACT

ANALYZING DIFFERENCES IN COLOR VARIATION SENSITIVITY BETWEEN EXPERTS AND NOVICES TO FIND A DIFFERENTIATING PROCESS IN PIGMENTED SKIN LESION DIAGNOSIS

Publication No. _____

Yu-Chin Chai, M.S.

The University of Texas at Arlington, 2007

Supervising Professor: Manfred Huber

Fatal skin lesions, such as melanomas, appear to have high color variation to experts but often as having low variation to novices. This thesis attempts to find whether it is possible to find a function representing an expert's color variation sensitivity to skin lesions without explicitly requiring them to provide rules or even a diagnosis. Various pigmented skin patch images with either normal pigmentation or with diseased lesions were evaluated by the participants, both experts and novices. Initial comparisons in various color spaces showed that only the RGB model confirmed the expectation that the experts' judgments represented the actual variation of the color whereas the judgment of novices seemed to be based on more than simply color

variation. To determine the best color space for lesion differentiation, an optimization process based on parametric color dimensions in an RGB color space was used to find the parameters of a color transformation function that best differentiated the color variation sensitivity between experts' and novices'. The analysis of results showed that this process was able to maximize the differences between the expert and novice's color variation sensitivity and to provide a criterion to discriminate between images of non-invasion and melanoma type skin lesions.

TABLE OF CONTENTS

LIST OF ILLUSTRATIONS

LIST OF TABLES

CHAPTER I

INTRODUCTION

Perceptual sensitivity to the color variation in skin lesions holds an interesting promise since differentiating color variation on visible skin lesions is an important ability to categorize and diagnose skin related diseases [7], [8], [64], [73], [77], [78] . Yet, to most average people, those colors often appear to be highly similar [47], [59], [60]. A skin lesion is a visible patch of the skin that does not resemble the area surrounding it [7], [42]. However, the color variation within it, such as the one between red and brown, are often categorized as low by people who have no experience or who have not received medical training concerning skin lesion diagnosis (they are aware of their skin lesion problems and consult with physicians). In other words, novices consider that those colors as similar. For instance, the study in color discrimination showed that color judgments of college students with stimuli containing red-brown color pairs resulted in a much poorer color differentiation than for other color pairs such as red and orange [25], [71].

Unfortunately, variation among those colors, such as red, brown, or dark brown, is one of the criteria to classify skin lesions [12], [66]. For example, a common way to differentiate paules or plaque (a patch of closely grouped papules) from other skin lesions such as pustule, telangiectasia, vesicle and wheal is to inspect the lesions' color variation (which often appear as pink, red and brown) along with other size and texture judgments [7], [18], [38]. Further more, high color variation is one diagnosis criteria for pigmented skin lesions (in the papules category),

such as, for example, malignant melanoma which can be fatal and for which the affected population is growing [63]. Melanoma often appears as having high color variation such as an uneven distribution and a mixture of colors of tan, brown, white, pink, red, gray, blue; and especially black across the mole, and is one of the indications for the possible progress of a morbid state of the melanocytes – the cells that produce pigment in the skin [1], [17], [18], [69], [73]. The concept of color variation seems to be straightforward, yet it is not easily learned for novices. Therefore, it is not surprising that without intensive education in the average population, most people often lack the sensitivity to distinguish lesions and are not aware that they should seek a medical opinion ([47], [59], [60], [63].)

Since a difference of sensitivity to color variation of skin lesions may exist between experts and novices, how can we find a function that shows the change of color variation sensitivity? The reason this function may be important is that most applications that state to apply human perception attributes do not separate the color sensitivity of experts and novices [9], [11], [13], [15], [19], [23], [49], [76], [81], [90], [91], [92], [98]. Or they simply assume that experts apply the same differentiation but only the weighting of rules for decision-making is different [24], [26], [101], [105]. Human perception seems to utilize visual information very efficiently. For instance, cognition and perception research shows that color constancy and object recognition in human visual perception seem to be able to tolerate significant variation in parameters such as luminance [67], [79], [82], [100]. Further more, if the data contain some irrelevant color features such as hair or an ink mark with similar colors as lesions, it could be fairly easy for the human visual system to tell the features apart from the lesion, while it requires a complex algorithm for the computer to differentiate them [45], [54], [84]. Efforts have been

made in the past to simulate human perception. The color variation, in terms of image analysis, can be measured by counting the number of colors, edges from luminance contrast, texture segments, etc. These tools have been applied to judgments in skin lesions, such as identifying the color representation in an image analysis approach or to directly use color attributes as part of an expert diagnosis system [31], [37], [39], [72], [78], [83].

In order to capture aspects of human color perception, an algorithm needs to be used to find the feature space that captures the vision system's properties. Two approaches of the use of color in skin lesion analysis have been implemented in the past [31], [32], [37]. The first approach is to use color directly by quantizing the color variation based on image analysis. This is used since some research suggests that color can be an effective way to identify an object or an property of the object [9], [11], [13], [19], [22], [23], [29], [76], [81], [90], [91], [92], [98]. Many applications aim to quantize the color variation such as segregating colors into different groups (color representations) that can be easily used to identify the region of interest (ROI) or the target objects for further uses [2], [4], [5], [68]. These methods followed the process: pre-processing the image to filter out noise [20], selecting a skin region to pre-cluster [16], and then processing the region of interest with different functions, to separate disjoint regions, to smoothen, or to find a proper region assignment label for each pixel region [53], [56], [57]. The second approach is to apply all color attributes, such as mean, variance, or other color space parameters such as saturation, as a part of an expert system and to use high-level logic to determine the weight of the attributes for further use, such as for performing a diagnosis on the skin lesion [14], [24], [26], [101] ,[104], [105].

The perception theories that were applied to color variation algorithms are often under debate in the field of perception. For instance, some algorithms that applied these theories pre-measured homogeneity of each pixel color to construct two subsets in the color space map [74], [80]. But other studies suggest that the human visual system has different color perception sensitivity depending on the spatial color distribution in the image [94], [106]. Some studies applied generic mechanisms, such as attention [44], to manipulate the weight of each perceptual attribute. However, these mechanisms are still debated in neural and cognitive studies (e.g., [65] , [97]), and it is hard to evaluate the process. Edges from luminance contrast studies can be varied due to different algorithms or formulas used [6], [19], [34]. But some research has shown that the number of surfaces and the number of colors could influence how we perceive objects [99]. Some methods that apply color perception mechanisms require pre-processing information that uses skin color as a baseline [33], [61]. However, the human perception system does not. Moreover, all of these algorithms, in particular if applied to the human perception approach, would in practice require prior knowledge of some artifacts as part of their implementation to implement the algorithms.

Why is it hard to find a right human perception model to simulate the skin lesion diagnosis process? In essence, a computer system has a different way to handle visual information as compared to the human perception system. For instance, a computer system with 24-bit displays is capable of displaying over 16 million colors; but not every single digitized color pixel is meaningful to the human visual perception system. Hence, high color variation can have an entirely different meaning from a computer and to a human [62].

Can we find a function that directly represents the pattern of the original human color variation behavior data? Can we use that function to perform the color variation measurements such that the outcome could show the way the perception system reacts to the stimuli in the task? In neuroscience, researchers attempt to retrieve the perception function based on optimizing the signal generated from a cell's response to the stimulus provided by the probe of the electrode (e.g. [27]). In this thesis, I employed a similar optimization approach but focused on expert color judgment rather than neural measurements. The first part of the work is to identify the strongest shift in the color variation judgment task between experts and novices. Since experts' and novices' color variation sensitivities are different, the possible shift can be strong enough to be observed in human behavior data. Hence, Chapter 2 lays out a pilot test that was done in order to collect data of experts' and novices' color variation judgment to a set of skin lesion images, containing images with normal pigmentation and skin lesion.

Chapter 3 focuses on establishing an optimization process in order to use differences between experts and novices to explore the possible parameters that represented the function that differentiated most between the color variation sensitivity of experts and novices. The general discussion is provided in the last chapter of the thesis to conclude the findings and possible introduce applications in the future.

CHAPTER II

PILOT STUDY

An expert is expected to have a higher sensitivity to the appearance of skin lesions then a novice [30]. One reason for such an enhanced sensitivity is that the color perception of an expert is tuned to a particular color domain and that perceptual sensitivity to the particular color stimuli can be expressed as a function of a particular dimension in a color space. To determine whether or not this might be the case, the first step is to sample the individual's response to the stimuli that occur as part of the expert's daily routines. In the study presented here, images containing skin lesions were used for the evaluation. The pilot study in this project was a human experiment in which the expert and novice participants were asked to evaluate the color variation on a set of skin lesion images without involving any diagnosis or judgment as to what type of lesions were actually presented. In other words, the participant only needed to concentrate on how high or how low the color variation in the images was.

To gain a better sense of how individuals' perceived color variation, various color space models were applied to the images and correlation tests with the judgments of the human participants were performed. Each image was originally a digitized RGB image. For each of the used color space models, a transformation function was applied to transfer the RGB image values into the particular color space. The various color space models included were RGB, HSV, HSL, CIELab, CIExyz, CIExyy', CIELch and CIEuvl [28].

2.1 Color Space Models

Each color space model has its unique way to represent the color distribution in various dimensions. The RGB color model is an additive model where Red, Green and Blue, the primary colors, can be mixed in various ways to produce other colors. The primary colors are based on biological features because they are related to the differences between the physiological responses of the cone cells of the retina to the light spectrum. In addition, the RGB model is a three-dimensional orthogonal space and can therefore be easily associated with a Euclidean distance function. The main problem with RGB is that the distance between two points in the space has no relation to the closeness of the corresponding colors in human perception. In other words, it is not perceptually uniform [36].

Most color space models were defined by the CIE (the International Commission on Illumination) and work by weighting the visual spectrum [36]. Considering brightness and chromaticity as factors in color perception, where white and grey have the same chromaticity and only the degree of the brightness is different, CIExyz was created. The y parameter in the CIExyz color space is a measure of the brightness of a color. The other dimensions in CIExyz define the space of the colors that should be distinguishable by a human. However, CIExyz provides a perceptually non-uniform color space. On the other hand, two other CIE color models, CIELab and CIELuv, are perceptually uniform.

CIELab is commonly used since it is to be device independent, meaning that the ratio of the color values do not change because of a change of the camera, video, or monitor. In addition, it is expected to be perceptually linear where a change of the same amount in a color value should match a change of the same visual attribute in human perception. The three parameters L,

a, and b in the model represent the luminance of the color (L=0 yields black and L=100 indicates white), its position between magenta and green (a, where negative values indicate green while positive values indicate magenta), and its position between yellow and blue (b, where negative values indicate blue and positive values indicated yellow). CIELab has no associated two dimensional chromaticity diagrams and no correlate to saturation. In a similar approach, CIELuv is also device independent and perceptually uniform but has an associated chromaticity diagram, a two dimensional chart where the color is determined as an additive mixture. CIELch and CIExyy' are modified versions of CIELab and CIExyz, respectively. A brief comparison, adopted from Mathwroks [88] is as follows:

RGB: uses Color matching curves R=700 nm, G=546.1 nm, B=435.8 nm;

CIExyz: y = Luminescence (cd/m^2); x, z = spectral weighting curves;

CIExyy': y' = Luminescence (cd/m^2); x, y = chromaticity coordinates;

CIELab: L = Luminescence (density); a = red/green; b = blue/yellow;

CIELuv: L = Luminescence; u = saturation; v = hue angle;

CIELch: L = Luminescence; c = chromacity; h = hue angle.

The HSV (Hue, Saturation, Value) model, also known as HSB (Hue, Saturation, Brightness), defines a color space as a nonlinear transformation of the RGB color space. In particular, Hue specifies the dominant wavelength of the color, except in the range between red and indigo in which Hue denotes a position along the line of pure purples. In HSV, value stands for the maximum amplitude of the light waveform whereas in HSL, also known as HIS (another

similar but slightly different color space model), L stands for luminance (I stands for intensity) in a more detailed sense. In HSL, the chromaticity diagram is a double cone with black and white points placed at the two apexes of the double cone, whereas in HSV it is a single cone. Both HSV and HSL were applied in this thesis for the color space correlation testing as well as other CIE system color models.

2.2 Color Sensitivity Evaluation

Two measurement variables, the mean (centroid) and the standard deviation (variation) of each color space model were observed in the correlation test. The expectation was that significant correlations could be observed between an expert's color variation judgment and only the color variation variables, whereas the novice's color judgment would correlate with both measurement variables. According to the literature, rather than applying all possible rules toward judgments, experts often apply only a few rules that are efficient enough to make a decision [3], [10], [35], [52]. Two perspectives were taken in the color space model correlation tests. First, to judge the color variations, an expert's evaluation should be correlated more with the variation and correlated less with the other unrelated measures such as the average value of the colors. Second, the correlation tests reveal which color space fits the expectation.

2.3 Methods

2.3.1 Participants

Six adults voluntarily participated in the experiment. Three dermatologists, two males and one female, from Southwestern Medical Center at Dallas were recruited as experts and three undergraduate students, two males and one female, from the Department of Biology, University of Texas at Arlington were recruited as novices.

A pre-screen test was run to ensure that the stimuli were useable and the experimental process was valid before the main experiments were run. Six graduate students, including the author from the Department of Psychology, University of Texas at Arlington were additionally tested in 2003.

2.3.2 Stimuli and Apparatus

Ninety-four images containing various skin lesions or regular pigmented patterns such as moles were used in the project. Each image was resized to 1x1 inch and stored as a 24-bit RGB image, where the red, green and blue components were 8 bits each. For experimental control purpose, when resizing the image, the image region used was such that each lesion/mole was centered as closely as possible within the images. In addition, resizing made sure that the surround of the lesion was visible and no part of the lesion was missing. Eighty-two images, similar to the ones shown in Figure 1, were used for color variation evaluations in this pilot study, and twelve images served for the purpose of validation in the optimizing process. Appendix B lists the diagnosis in detail. Note, that due to the limited availability of images, only sixty-three images contained the diagnosis from a physician, the rest of the images were pigmented patterns of skin, such as moles. For the later optimization process, which will be discussed thoroughly in Chapter 3, the images were grouped into three categories: non-invasion patterns (labeled as non-invasion), early sign of a possible melanoma (labeled as early-sign), and melanoma (labeled as melanoma) [46], [102]. Melanoma refers to the type of skin lesion that has developed into the late stage of cancer. The early-sign group indicates the group of lesions with signs that there is a chance for them to develop into skin cancer. The non-invasion group indicates that there is no sign for invasion developed and that they likely are no harm or threat to

the owner. Note that in the pilot study the stimuli were presented ungrouped and the color images were printed on A4 sized white paper. Twenty-five images were printed per sheet of paper. Each participant evaluated about four pages as to the perceived color variation in each image and gave the evaluations on a separate sheet. Each image of each survey sheet was numbered and participants rated the color variation accordingly.

(a) (b)

Figure 1 Sample stimuli used in the human color variation judgment study where Figure 1.a. represents a regular mole and Figure 1.b. a melanoma type skin lesion. Note that both pigmentations seem to be similar but Figure 1.b contains a higher color variation in a clinical view.

2.3.3 Design and Procedure

Most human color perception experiments have been done in the laboratory with a specific viewing time constraint, usually as short as a hundred milliseconds, due to various hypothesis-testing reasons. This is the case, in particular when the research interest is geared towards understanding the interaction between luminance and color interactions [21] in the visual perception system. In real life, however, even if the observer's viewing time is longer than under laboratory control, we are still able to maintain our color constancy to some degree. King [48] suggested that a moderate viewing time could improve the rate of discrimination of the targets. Hence, the duration of the experiment performed here was selected to be not too short.

On the other hand, it was also not too long in order to prevent people from either underrating or overrating the color variations. The whole experiment lasted for about 10 to 15 minutes depending on individual needs. The task of the experiment was to evaluate the color variation where the response to each image was discretized to a three-point scale (low, medium or high). In addition, the instructions stated not to pay attention to the parts of the image that did not belong to lesions, such as hair and lighting conditions. Each participant, including pre-screen participants, received a consent form to inform them of their rights as a participant in the experiment and signed consent forms were collected. A brief debriefing session was provided after the experiment.

Although the survey responses could be scaled to a hundred-point scale, previous expert and decision making studies (e.g. [3], [10]) indicate that humans, even experts, tend to make a rough decision even when many variables are presented. In other words, humans judge the information base on rank order instead of precise numbers. Therefore, instead of showing a scale of 1 to 100, the survey only obtained a 4-point scale: none, low, median and large as a typical decision making scale. However, since there were no images in the set that could have warranted a choice of no variation, the survey was designed as a 3-point scale. To analyze the results, color space model transformations were using color conversion functions from the Matlab image processing toolbox. For the transformation formulas, please refer to Appendix A.

2.4 Results

A correlation test was applied in order to measure the strength of the associations between human evaluations and metrics (mean or standard deviation) of various color space dimensions. Since there was no assumption that the population of the images was from a normal

(Gaussian) distribution, and because the sample size was small (n=3), a nonparametric coefficient correlation test, Spearman's rank correlation was used. Spearman's rank correlation coefficient 'r' was proposed by Spearman in 1904 as a measure of linear association and defined as follows:

$r' = 1 - 6\sum \frac{d^2}{N(N^2 - 1)'}$ where d is the difference of the corresponding variables

, and N is the sample size

A dummy code of 1, 2, or 3 was applied to encode the rank order of low, medium or high, respectively. Table 1 shows the results of Spearman's rank correlation coefficient association strength between the standard deviation and the mean values of RGB color space model and the color variance evaluations obtained from the experts and novices. ** indicates that the *p* value is less than 0.01, and * indicates that the *p* value is less than 0.05.

As Table1 shows, Spearman's rank correlation coefficient shows overall significant associations between experts' color variation judgment and standard deviation of RGB color dimensions, but not each dimension is significantly correlated with every expert's color variation judgment. Only the standard deviation of the R dimension is significantly correlated for all experts. The correlation coefficient is significant between two novices' color variation judgment and standard deviation of RGB color dimensions, and one novice's color variation judgment does not show significant association with any RGB color dimensions.

The correlation coefficient showed no significant association between experts' color variation judgment and the mean of RGB color dimensions. However, the correlation coefficient showed significant association between novice 2 (N2)'s color variation judgment and the mean

of the B color dimension, and between novice 3 (N3)'s color variation judgment and the mean of the G color dimension.

The results in the RGB model, fit the expectation involving expert and novice color variation judgments, where experts had no correlation with the mean color value but with the standard deviation value. Novices either had no correlation to any one of factors or had correlations to both the mean and the standard deviation. For the rest of the conventional color space models, however, none of the results fit the expectation as well as for the RGB model. Please refer to Appendix C for details.

Table 1 Spearman's rank correlation coefficient test on the association strength between the standard deviation, the mean values of the RGB color space model, and the color variance evaluations obtained from the experts and novices

	Color Variation (STD)			Color Centroid (Mean)		
	R	G	B	R	G	B
Expert						
E1	.421(**)	.315(**)	.149	.109	.175	-.012
E2	.350(**)	.143	-.026	-.069	-.002	-.194
E3	.738(**)	.438(**)	.346(**)	-.101	.038	-.178
Novice						
N1	-.106	-.013	-.100	.020	.067	.075
N2	.788(**)	.484(**)	.320(**)	-.159	-.010	-.229(*)
N3	.518(**)	.534(**)	.453(**)	.215	.356(**)	.208

** indicates $p<0.01$, *indicates $p<0.05$

2.5 Discussion

The experiment divided the color variation of the skin lesion into high, medium and low with respect to experts' and novices' judgments. The RGB model showed a pattern that fit the expectation that experts used fewer rules to achieve the judgments and in particular that it was more closely aligned with objective color variation. The results of the study also showed that color judgments among individuals were not uniform, which confirmed other color perception studies in psychophysics [50].

This study did not show the quantitative difference of the sensitivity between experts and novices to particular color stimuli (skin lesions) and the correlation test was weak to conclude whether the color variation sensitivity shifts due to the stimuli. Chapter 3 develops a process that was able to differentiate the color variation sensitivity between the experts and novices to evaluate if this difference could be correlated to the measurements used in the diagnosis making tasks that the expert performs.

CHAPTER III

OPTIMIZATION PROCESS

Human color variation judgments in the pilot study showed that the experts' judgments correlated with color variations in RGB color space in general. However, the correlation study did not answer what the color variation sensitivity function of the expert was and whether it directly reflected sensitivities based on the diagnosis ability of pathological differences or not. One way to determine an expert's sensitivity is to change the color dimensions in the color space and observe how well the behavior data from color variation judgments correlate with it. The typical ways of determining those parameters in the past were either to directly apply the parametric dimension in the color spaces that was claimed to be closest to the human perceptual color space, or to start from a set of equal parameters and then to apply other classifies functions such as clustering techniques to group the values according to the color representation (e.g. [103]). In general, human evaluation was then the last stage in order to be used to validate the outcome that the computer generated. The human judgment could here be artificially biased since the set of stimuli had been automatically determined by the computer. For instance, in Celebi et. al. [13] human experts validated images that contained color segmentation generated from various algorithms by responding *how close* to the experts' ideal color segmentations the results were. The pattern, however,

was not the same as the pattern by which the experts thought the segmentation should have been generated.

One way to find a generic pattern is to apply an optimization process to classify the behavior data. This method has been applied in the biomedical engineering field (e.g. [27]), where the research applies an optimization function to classify the sequential signal wave generated from a cell reacting to an electrode (the stimuli). A similar approach was adopted in this project where the optimization process is based on the color variation judgments for the particular stimuli (skin lesions).

(a) (b) (c)

Figure 2 Sample images of examples of the three image groups: (a) non-invasion (b) early sign (c) melanoma

To determine the optimized parameters of a color transformation function that presents the strongest shift in color variation sensitivity between experts and novices, an optimization process was implemented, and the details of this process are discussed later in this chapter. The images were grouped into three diagnosis groups [42], [46], [77], [85] to evaluate the final results of the optimization process [7]. Figure 2 shows example images of three target groups which represented non-invasion, early sign of invasive lesion, and final state of melanoma, based on the clinical diagnosis that labeled

the image [42], [46], [77], [85]. Non-invasion in general means a normal pigmentation and contains no information of abnormal cell growth activity. Early sign denotes that the appearance of the skin lesion may contain some suspicious and abnormal patterns that indicating the possible progression towards skin cancer such as melanoma [46]. Those lesions, however, required further examination to exclude or include the possibility of cancer development. The melanoma type images indicated the images contain the lesions that have reached the final stage of melanoma development; and intensive medical intervention is usually required at this stage to observe and prevent the abnormal cells from invading neighboring tissues or even organs.

A complete diagram of the optimization process is shown in Figures 3, 4 and 5. The whole optimization process includes optimizing the color transformation to determine the strongest parameters for a color variation sensitivity function, color retransformation with the optimized parameters, and a validation process.

3.1 Finding a Color Validation Model for Novice to Expert Color Sensitivity Shift

3.1.1 Color Variation Measurement and Color Space Transformation

The first step of the optimization process is to assign a set of arbitrary parameters for parametric color dimensions in RGB color space. Figure 3 shows the component that calculates a value of color variation for a given lesion image by applying a parametric color transformation, followed by a variation metric. This component is central to the initial optimization and is also applied with the optimized

parameters to the determination of potential diagnosis rules and in the validation process.

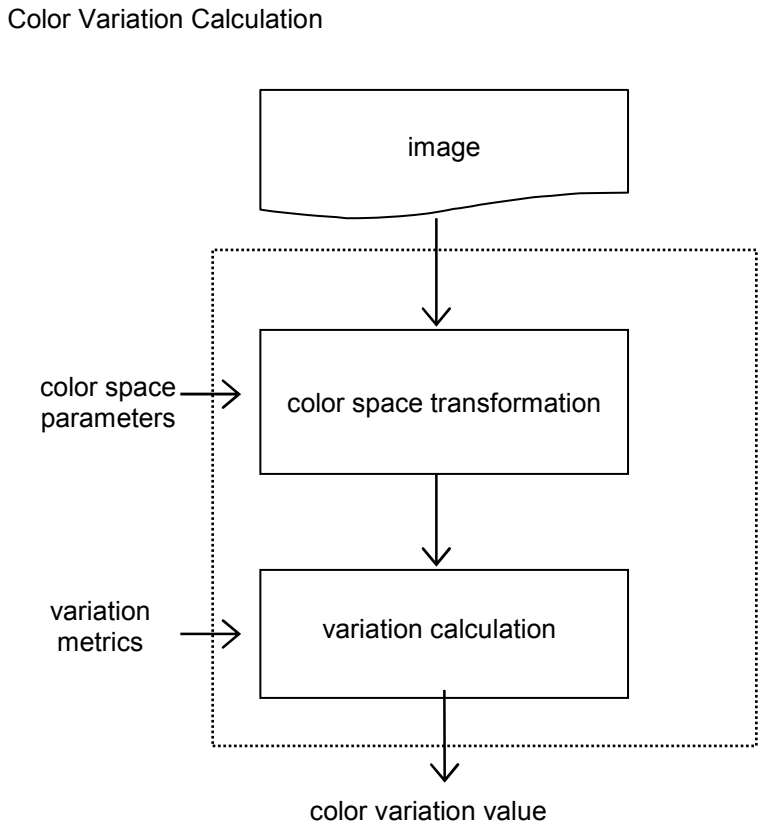

Figure 3 The color variation calculation using a parametric color transformation process and a selectable variation metric

A color image of size M x N is defined in terms of three sequential elements

$$r(m, n),\ 1 \le m \le M;\ 1 \le n \le N$$

$$g(m, n),\ 1 \le m \le M;\ 1 \le n \le N$$

$$b(m, n),\ 1 \le m \le M;\ 1 \le n \le N$$

where each element represents with the R, G and B component at location (m, n) in the image. In the images, each individual color component was presented using 8-bits and thus each element was an integer between 0 and 255 which was then normalized to a value between 0 and 1. The pilot study and the experiments modified the images to be of size 1 x 1 inch with a resolution of 72 x 72 pixels. In human perception, the variation of the chromatic information may follow a linear relationship as suggested in human color studies [43]. Hence, a linear function for transforming the RGB color space was adopted for the purpose of changing the selected color dimension:

$$i(m,n) = \frac{a * r(m,n) + b * g(m,n) + c * b(m,n)}{a + b + c}$$

where r, g, b, stand for the base colors in the RGB model normalized between 0 and 1. *a*, *b*, and c, stand for the transformation parameters that ranged from 0 to 10 in increments of 0.1. *i* represents the color transformed intensity image. The process generates a color value for each pixel as a function of the image and the parameters. The color variation in the given color dimension is then calculated using a variation metric. Metrics used here were the mean, standard deviation, and the expected value of the spatial frequency. The reason for the spatial frequency in addition to the other metrics was that the sensitivity to texture information might be an important factor in color variation judgment. To be able to evaluate texture in this component, it was represented as a summarized representation of the spatial frequency domain. To determine this spatial frequency metric, we employed a two-dimensional discrete Fourier transformation. In order to summarize the transformed spectrum of each image

into a single value that could be correlated to the data point of the human judgment, the expected value of the spatial frequency was computed as follows. A two-dimensional discrete Fourier transformation calculated the amplitude A(m, n) for spatial frequency components with horizontal index (m) and vertical index (n), where the horizontal frequency is (π* i)/ m and the vertical frequency is (π* i)/ n. Because amplitudes are symmetric around π and A(π, k) = A(-π, k), only spatial frequencies between 0 and π are used. By using these horizontal and vertical components a spatial frequency index, f, can be computed as

$$f(m,n) = \sqrt{m^2 + n^2}$$

and its expected value is given by

$$E(f) = \sum_{f} P(f) f = \frac{\sum_{m=0}^{M-1} \sum_{n=0}^{N-1} A(m,n) * f(m,n)}{\sum_{m=0}^{M-1} \sum_{n=0}^{N-1} A(m,n)}$$

E(f) is here the expected value of spatial frequency index and serve to generate a single value for the correlation computation.

3.1.2 Color Variation Measure Optimization

As shown in Figure 4, the set of variation metrics introduced in the previous section were used to compute a variation value for each image and the resulting values were correlated using Spearman's correlation with each participant's color variation

rank-order judgment. The transformation was enclosed in an optimization function [41], [51] using a simplex approach in an n-dimensional space characterized by n+1 distinct vectors. In each search step, the optimization function generates a new point of parameter vector in or near the current simplex and the function value at the new point is compared with the previous values. This step is repeated until the diameter of the simplex is less than a local minimum near the vector.

The differences between experts' and novices' color variation sensitivity were calculated as the difference between the average correlation value of the experts and the average correlation value of the novices.

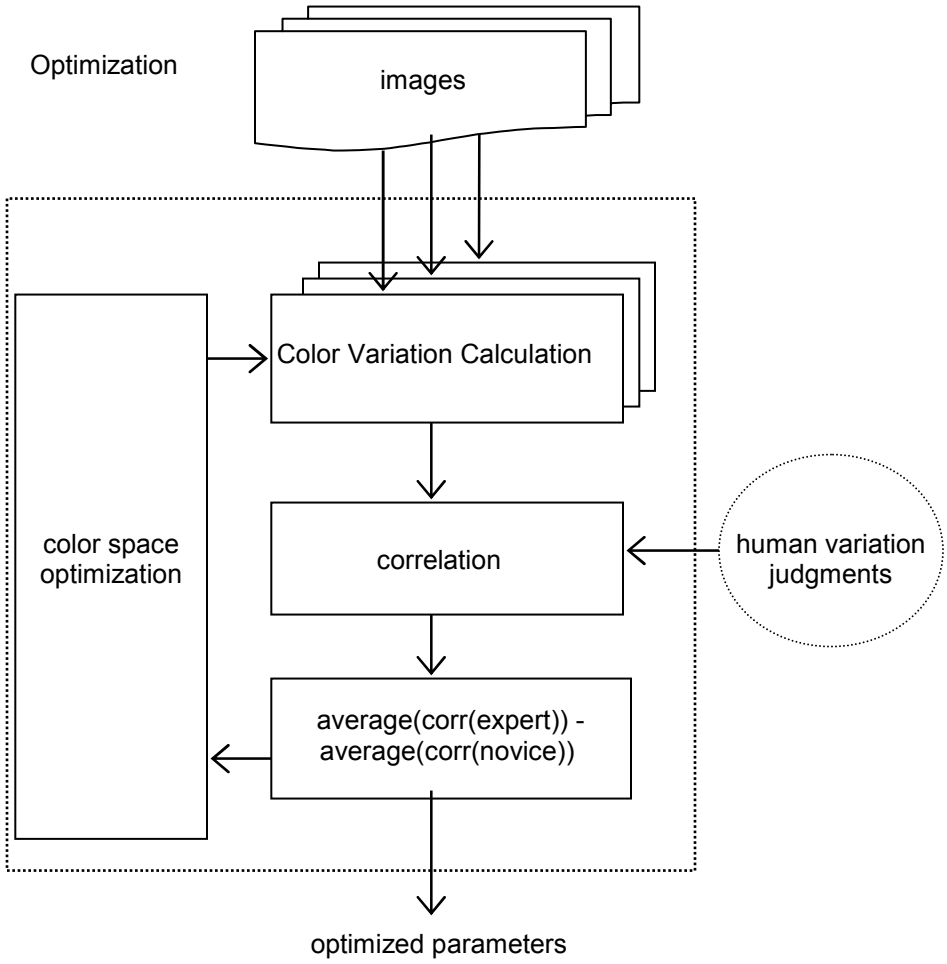

Figure 4 The optimization process for finding optimized color transformation parameters

3.2 Diagnosis Function and Validation

Once the optimized parameters were generated, the parameters were used in the color variation calculation with the same set of images to determine and validate potential diagnostic rules as shown in Figure 5.

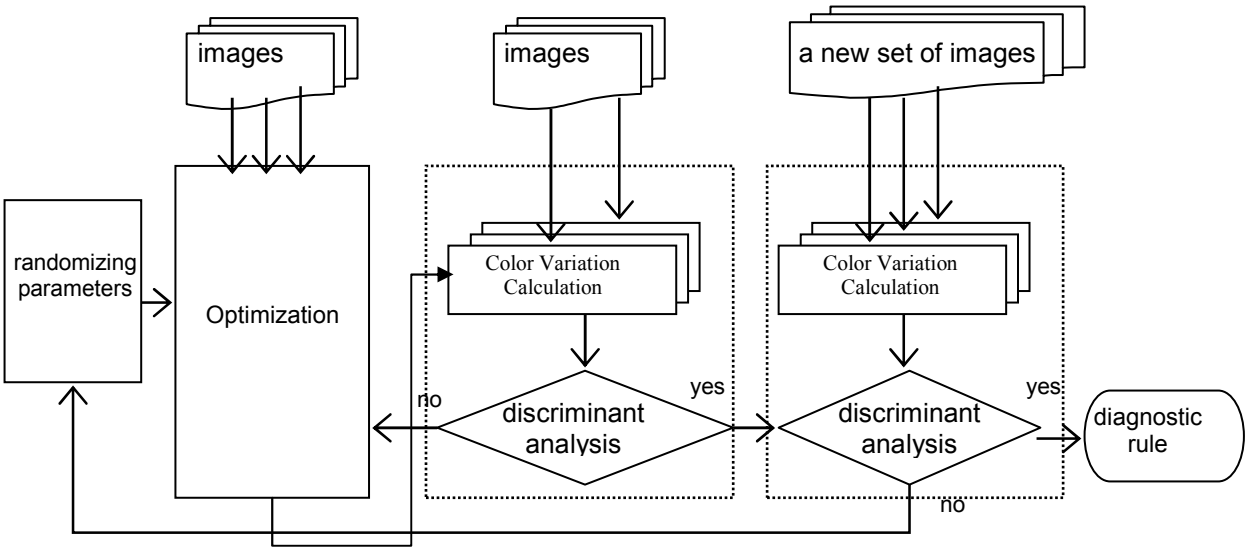

Figure 5 The complete optimization process

3.2.1 Diagnosis Function

The process used to find a potential diagnosis functions list generated a set of color variation values for the optimized color dimension and then a discriminant analysis was applied to these values to test if they identified significant differences between skin lesion groups. The discriminant analysis is a statistical analysis method that shows how far groups are apart in terms of the given measure [58], [95]. m groups here can be represented as $a+b_1* X_1+ b_2* X_2+\ldots+ b_m*X_m$, where a is a constant,

X_1, X_2, …, X_m are the numeric group labels, and b_1, b_2, …, b_m are the correlation coefficient values, the standard beta value. Discriminant analysis uses the beta values to compute the canonical correlations. The main use of discriminant analysis is to predict group membership from a set of predictors. Accordingly, an attempt is made to delineate based upon maximizing between-group variance while minimizing within-group variance. The Wilks' Lambda is used to reflect variable's importance. The smaller the Wilks' Lambda, the more important the variable is. Therefore, the smallest Wilks' Lambda and the greatest significance relate to the most important variable. In general, canonical correlations of magnitude $R \geq .30$ may become statistically significant. In this application, m is 3, and based on the original diagnosis, the images were sorted into non-invasion, early sign and melanoma. Based on the canonical correlation value, Wilks' Lambda test was applied to test the significance of the difference between these groups. As part of this process, it is required to assign numeric group label, in order to calculate how the clusters for each group can be differentiated and if they are significantly different from each other. In this case, non-invasion images were identified as group 1, early-sign as group 2, and melanoma as group 3. Since a color variation value corresponded to each image, the significance test determined whether the optimized parameters, found by determining the transformation that maximized the transformed the maximum difference between experts and novices in terms of their color variation judgments, allowed to differentiate between non-invasion lesions, possible early–sign of invasion, and melanoma images.

3.2.2 Validation Process

In order to verify that the function could serve to aid in the diagnosis of the lesion types, as shown in Figure 5, the validation process was the next step, once the significant values were found in the discriminant process. Here, six images per group were assigned which were not evaluated in the pilot study before. However, due to the shortage of early sign images, only the non-invasion and the melanoma groups were available as validation targets. The same discriminant analysis was then applied. Once a significant difference was shown, the process could stop as a set of optimized parameters and a significant diagnostic rule was found. However, due to the explorative interest, the whole optimization process may restart to search for more potential solutions (functions) as the goal stated.

3.3 Experiment

To implement the complete optimization process, parameters of the color transformation were initially assigned randomly, ranging from 0 to 10 in increments of 0.1. The optimized parameters for the color variation measurement, including a color variation metric, were then calculated to optimize the difference between the correlation between the calculated color variations and the color variation judgments of experts and novices based on the assigned parameters. The optimized parameters and the same color variation calculation process was then used to generate a set of color variation values from the new color space and these values were applied to the discriminant analysis to test the significance of their ability to differentiate between skin lesions groups. Once significant values were found, meaning that the canonical correlation was high and

Wilks' Lambda test showed that p was smaller than chance at a level of 0.05, meaning that it was unlikely that it could have been caused by chance, the validation process was performed. The validation process was similar to the process applied in the previous discriminant analysis except that it used a set of images that were not evaluated in the pilot study. This discriminant analysis was used to confirm that the color transformation function with optimized parameters was able to generalize the outcome to images that were not included in the group that produced optimized parameters. Once a significant difference was shown, the process could stop as a set of optimized parameters and a potential diagnostic rule was found.

3.4 Results and Discussions

The process revealed two functions that significantly differentiated skin lesion groups. The highest was the primary color R in RGB color space. The second was reached from the initial parameter set a=1.0, b=0.1, c=0.5 as a set of optimized parameters 1.632, 0.099, 0.357 in the linear function.

Visualization graphs showing centroids of the groups were used to report the distance between groups and Figures 6 and 7 presented how far the used variation measures allowed those grouped to be moved visually apart from each other.

R, with the standard deviation as metric, was significant, where the optimized parameters were equal to 1, 0, 0, resulting in a canonical correlation of 0.530, and a Wilks' lambda of 0.730 (p<0.001). Further comparisons showed that the melanoma group was significantly different (centroid= 1.016) from the non invasion group (centroid=-0.372, p<0.001), and from the early-sign group (centroid=-0.323, p<0.01).

Please refer to Figure 6 for the distribution of cluster centroids. There was no significant differentiation between the non-invasion group and the early sign group with a canonical correlation of 0.010 (p=0.949). The validation process showed that the non-invasion (centroid=-0.690) and melanoma (centroid=0.690) groups were different with a canonical correlation of 0.603 and Wilks' Lambda of 0.636 (p<0.05).

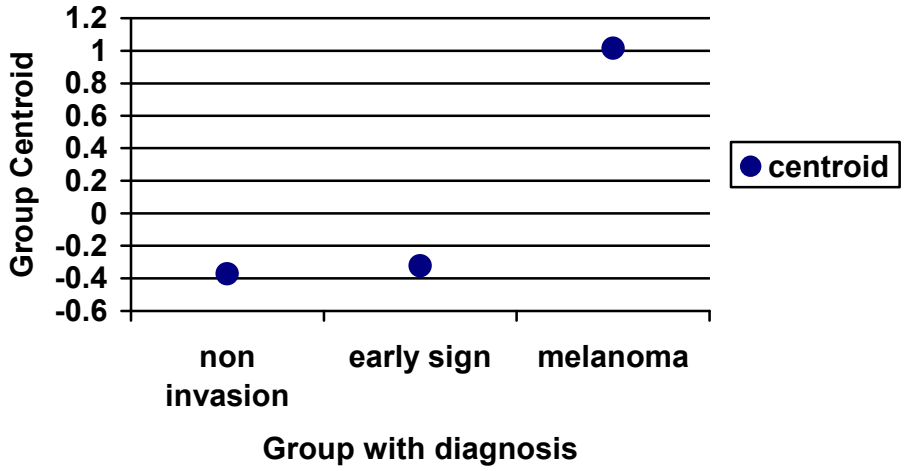

(a)

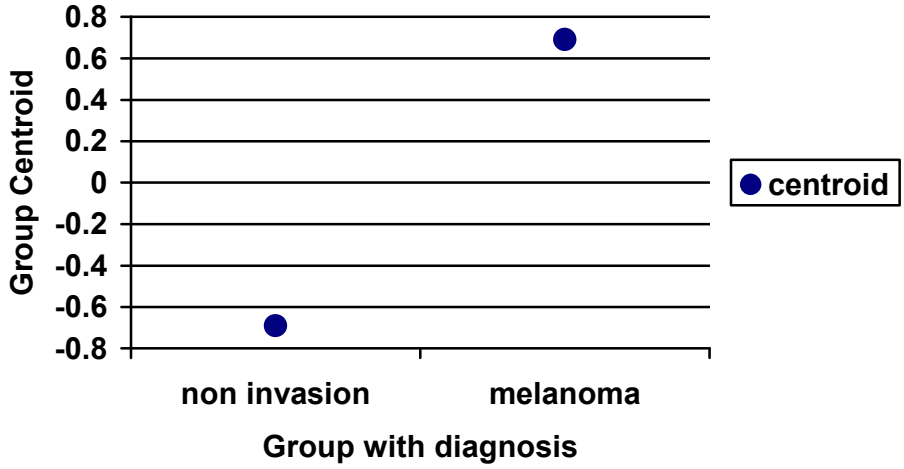

(b)

Figure 6 The results of discriminant analysis with the color transformation function, *i*= R. (a) shows the cluster centers (b) shows the cluster centers for the new validation image set

The linear function with parameters a=1.632, b=0.099, c=0.357, and using standard deviation as the validation metric resulted in a canonical correlation of 0.491 and Wilks' lambda of 0.759 ($p<0.001$). A further comparison showed that melanoma was significantly (centroid= 0.950) different from the non-invasion group (centroid=-0.362, $p<0.001$) and the early-sign group (centroid=-0.279, $p<0.01$). Please refer to Figure 7 for the distribution of cluster centroids. There was no significant differentiation between the non-invasion group and the early-sign group (canonical correlation=0.047, $p=0.749$). The validation process showed that color variation values were different between the non-invasion (centroid=-0.661) and the melanoma (centroid=0.661) groups with a canonical correlation of 0.587 and Wilks' lambda of 0.656 ($p<0.05$). There was no significant difference in mean or expected value of spatial frequency for both functions.

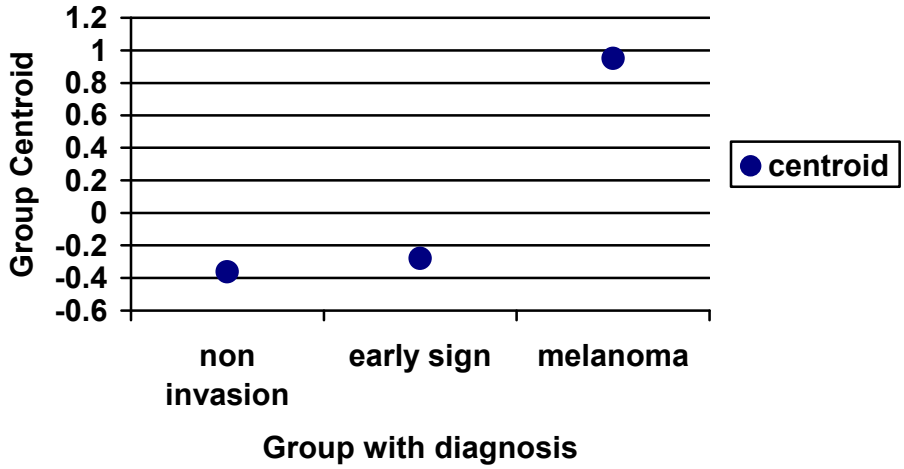

(a)

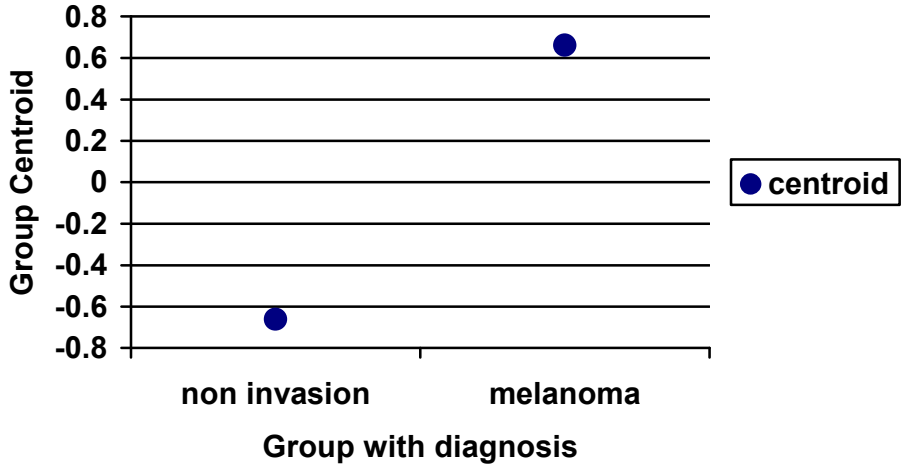

(b)

Figure 7 The results of discriminant analysis with the optimized parameters a=1.632, b=0.099, c=0.357. (a) shows the cluster centers (b) shows the cluster centers for the new validation image set

In general, none of the optimized parameter sets for the mean or the expected value of spatial frequency metrics, resulted in rules with significant discrimination results. The highest canonical correlation values using the mean metric (canonical correlation = 0.237, p = 0.177) was found for the function with parameters 1, 0, 0. For the expected value of spatial frequency metric, the highest canonical correlation value (canonical correlation =0.264, p=0.114) was found for the function with parameters 1.0, 0, 1.0. No further function was found even in G and B alone. As Table 2 shows, the analysis of the results showed that the optimization process can differentiate the non-invasion from the melanoma group. The results implied that sensitivity to the variation of the R value could be one of the important diagnosis indices for experts and the results did not confirm the suggestions [40] that the G and B components differentiated the type of lesion but not the R value. However, this could be partially due to the limited diversity of early sign images where sample sizes were fairly small for each category.

Table 2 Comparisons of the results and selected common parameters in other color functions with the standard deviation metric

Studies	Functions	Canonical Correlation	p-value
optimized parameters	$\frac{1.0*R+0.0*G+0.0*B}{1.0+0.0+0.0}$	0.53	<0.001
optimized parameters	$\frac{1.63*R+0.09*G+0.36*B}{1.63+0.09+0.36}$	0.491	<0.001
Tseng, et al. (1992)	0.607R+0.174G+0.201B	0.210	0.079
Celebi et al. (2005)	1/3(R+G+B)	0.148	0.510
Round et. al. (1997)	1/2(2G-R-B)	0.010	0.949

As shown in Table 2, the results did not show any significant discrimination capability in the context of the standard deviations as a variation measure, when equally weighting the components of the RGB color space as some human perception based applications suggested. For instance, 1/3(R+G+B) (canonical correlation, as an abbreviation *c.c.*, = 0.148, p = 0.510) in the study of Celebi, et. al. [13], and r=R/(R+G+B); g=G/(R+G+B); b=B/(R+G+B) in the study of Umbaugh et. al. [90]. The parameter values were not close to the ones that some color applications suggested. For instance, the study of Tseng et. al. [89] applied the xyz model with the parameters as follows: 0.607R+0.174G+0.201B (c.c.=0.210, p=0.079); 0.299R+0.587G+0.114B (c.c. = 0.099, p = 0.506); 0.000R+0.066G+1.117B (c.c.= 0.047, p=0.749).

The optimized parameter set (1.63, 0.09, 0.36) is close to the parameter of x in the CIExyz color space model except that the parameter for G in the optimized model was lower (b/(a + b+ c)=0.05) and the value for R was correspondingly larger. However, the x dimension in the CIExyz performed significantly worse in the discrimination test. Similarly, the results were not close for the transformation function that the study in Round et. al. [76] suggested, (R-B) (c.c.=0.135, p= 0.577) or 1/2 (2G-R-B) (c.c.= 0.010, p= 0.949).

To show a visual comparison, the RGB values of two sample images were transformed with the optimized parameters and converted into gray scale with Photoshop 5.0's default grayscale conversion routine. For comparison purpose, two typical parameter sets from past color transformations were also used.

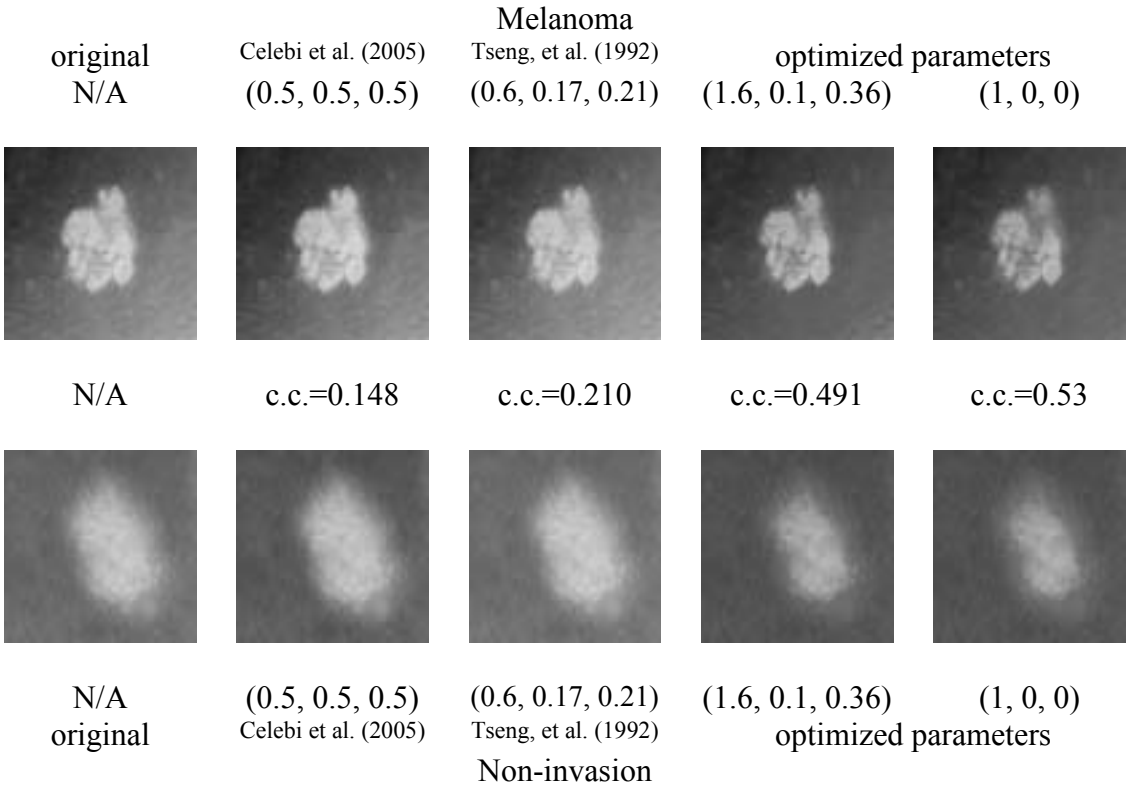

Figure 8 General comparisons of color transformation with typical methods and the optimized parameters in this study on both non-invasion lesions (bottom) and melanoma lesions (top). The values within the parentheses ( ) indicate the parameter values, 'c.c.' indicates the canonical correlation of the discriminant analysis where higher value indicates a better discriminant between non-invasion and melanoma

CHAPTER IV

CONCLUSIONS AND FUTURE WORK

This thesis showed that, without explicitly requiring experts to provide a diagnosis, the proposed optimization was capable of estimating a color sensitivity function based on the differences of experts' and novices' color variation judgment that was able to differentiate skin lesion types. A similar process can be expected to apply to help other expert-novice studies.

The color space correlation tests implied that human expert perception judgment would not utilize all the feature attributes at once [87]. In our case, expert color judgment was related to the color variation in RGB color space. The results showed that the strongest color variation sensitivity shift should use the R value as the dimension in RGB space. Parameters with (1.63, 0.09, 0.36) as a, b and c in the linear RGB transformation showed slightly less significant results compared with the color function then with R only. This set of parameters is similar to the x parameter in CIExyz color space model where a= 0.607, b= 0.174 and c=0.201. The difference between them was that the parameter b value was smaller than in the x parameter of the CIExyz color space.

However, even the best parameter set only differentiated melanoma from the rest. The subtle discrimination between non-invasion and early-sign was not found. This might be due to the large diagnosis diversity of the early sign group or due to the fact

that melanoma is the dominant factor in the shift which could cause the effect of the differences of color variation sensitivity between non-invasion and early-sign groups to be dominated (and thus hidden) in the regression test [86].

Several directions could be followed in the future development. First, the parameters may be extended as a function. A further computation model could be set to examine the potential range of the parameters or the function within it. In addition, several applications with direct diagnosis from experts ([55], [56], [57], [93]) suggest that for the purpose of categorization in detail, other knowledge rules are needed, such as size, symmetry and changes in lesion over time. The future direction of this project should extend to study how to combine higher decision making rules such as pain or the distribution of lesions for further diagnosis. Further, more precise control through an image registration technique is needed in order to ensure the quality of images and to reduce noise (e.g. [75]). Also, larger data sets should be included in future studies in order to examine the reliability of the process. Finally, it may be interesting to know how the color variation sensitivity changes through the growth of the lesion.

APPENDIX A

COLOR SPACE CONVERSIONS

Color Space Conversions

HSL

Based on the RGB color space, Max is the greatest of the (R, G, B) values, and Min is equal to the smallest of those values. The formula can be written as:

$$H=\begin{cases} \text{undefined}, & \text{if Max} = \text{Min}; \\ 60\text{degree x}\dfrac{G-B}{Max-Min}+0\text{ degree}, & \text{if Max} = \text{R and G} = \text{B}; \\ 60\text{degree x}\dfrac{G-B}{Max-Min}+360\text{ degree}, & \text{if Max} = \text{R and G} < \text{B}; \\ 60\text{degree x}\dfrac{B-R}{Max-Min}+120\text{ degree}, & \text{if Max} = \text{G}; \\ 60\text{degree x}\dfrac{R-G}{Max-Min}+240\text{ degree}, & \text{if Max} = \text{B} \end{cases}$$

$$S=\begin{cases} 0, & \text{if Min} = \text{Max}; \\ \dfrac{Max-Min}{Max+Min}=\dfrac{Max-Min}{2L}, & \text{if } 0 < \text{L} = 0.5; \\ \dfrac{Max-Min}{2-(Max+Min)}=\dfrac{Max-Min}{2-2L}, & \text{if L} > 0.5, \text{L} = 0.5(\text{Max} + \text{Min}) \end{cases}$$

HSV

H is the same as for HSL. L and V, however, are different.

$$S= \frac{Max-Min}{Max}=1-\frac{Min}{Max} \ ;$$

V= Max

CIExyz

$$\begin{bmatrix} x \\ y \\ z \end{bmatrix} = \begin{bmatrix} 0.412 & 0.358 & 0.180 \\ 0.213 & 0.715 & 0.072 \\ 0.019 & 0.119 & 0.951 \end{bmatrix} x \begin{bmatrix} R_{RGB} \\ G_{RGB} \\ B_{RGB} \end{bmatrix}$$

CIExyy'

Mathematically, *x* and *y* are projective coordinates

$$x = \frac{X}{X+Y+Z};$$
$$y = \frac{Y}{X+Y+Z},$$

where X, Y, Z are the parameters of CIExyz

$$y' = \frac{X}{xy}$$

CIELab

Mathematically, parameters L, a, and b are converted from parameters of CIExyz model

$$L = \begin{cases} 116\,(\,Y / Yn\,)\,1/3 - 16, \text{if } Y / Yn > 0.008856; \\ 903.3\,Y / Yn, \text{otherwise} \end{cases}$$

$$a = 500\,(\,f\,(\,X / Xn\,) - f\,(\,Y / Yn)\,)$$

$$b = 200\,(\,f\,(Y / Yn\,) - f\,(\,Z / Zn\,)\,), \text{where } f\,(\,t\,) = \begin{cases} t\,1/3, \text{for } t > 0.008856; \\ 7.787t + 16/166, \text{otherwise} \end{cases}$$

where Xn, Yn, Zn are referred to the white point meaning the number that produces white color.

CIELuv

Mathematically, parameters L, u, and v are converted from parameters of CIExyz model

$L = 116(Y / Yn)^{1/3} - 16$; $u = 13L (u' – un')$; $v = 13L (v' - vn')$

where Xn, Yn, Zn are referred to the white point meaning the number that produces white color. The quantities un' and vn' refer to the reference white point or the light source. (For example, for the 2° observer and illuminant C, un'= 0.2009, vn' = 0.4610.)

Equations for u' and v' are given below:

$$u' = 4X / (X +15Y + 3Z); \quad v' = 9Y / (X + 15Y + 3Z)$$

CIELch

Mathematically, parameters L, c, and h are converted from parameters of CIExyz model

$$C = (a^2 + b^2)^{1/2}$$

$$H = 0, \text{ if } a = 0; \quad H = (\arctan ((b) / (a)) + k * \pi / 2) / (2 * \pi) \text{ if } a \neq 0$$

$$\text{where} \begin{cases} k = 0 \text{ if } a \geq 0 \text{ and } b \geq 0; \\ k = 1 \text{ if } a > 0 \text{ and } b < 0; \\ k = 2 \text{ if } a < 0 \text{ and } b < 0; \\ k = 3 \text{ if } a < 0 \text{ and } b > 0 \end{cases}$$

APPENDIX B

IMAGE DIAGONOSES

a. The Diagnoses on the Images Used in the Study and Optimization

Non-invasion	# of images	Early-sign	# of images	Melanoma	# of images
Irritated Junctional N	2	Cmpd Dysplastic N	5	Melanoma	16
Junctional N	4	Compound N with mild dysplasia	3		
Compound N	5	Junctional Dyspl N	2		
Intradermal N & Lentigo Simplex	2	Dysplastic N	4		
Intradermal N	3	Dysplastic Compound N	1		
Junctional N w/lentiginous features	1	Cmpd N w/ architectural atypia	2		
Cmpd w/ lentiginous features	1	Dyspl N w/ Moderate Dyspl	1		
Benign Lentigo	2	Lentigenous Melanocytic hyperplasia w/ mild atypia	2		
Capillary Hemangioma	1	Lentiginous & Cmpd melanocytic dysplasia	1		
		Keratosis w/ lichenoid reaction & pigment incontinence	1		
		Cmpd N w/lentigenous melanocytic hyperplasia w/ mild atypia	2		
		Junctional N mild dysplasia w/o cytologic atypia	1		
Total	22		25		16

Note that N means Nevi

b. Images for the Validating on Process

Non-invasion	# of images	Melanoma	# of images
Intradermal N & Lentigo Simplex	1	Melanoma	6
Compound N	3		
Junctional N	2		
Total	6		6

Note that melanoma refers to the type of skin lesion that has developed into the late stage of cancer. The early- sign group indicates the group of lesions with signs that there is a chance for the development into skin cancer. The non-invasion group indicates that, no sign of invasion has developed and that they are likely no harm or threat to the owner.

APPENDIX C

COLOR SPACE WITH HUMAN JUDGMENT CORRELATION TEST

RGB

	Color Variation (STD)			Color Centroid (Mean)		
	R	G	B	R	G	B
Expert						
E1	.421(**)	.315(**)	.149	.109	.175	-.012
E2	.350(**)	.143	-.026	-.069	-.002	-.194
E3	.738(**)	.438(**)	.346(**)	-.101	.038	-.178
Novice						
N1	-.106	-.013	-.100	.020	.067	.075
N2	.788(**)	.484(**)	.320(**)	-.159	-.010	-.229(*)
N3	.518(**)	.534(**)	.453(**)	.215	.356(**)	.208

CIExyz

	Color Variation (STD)			Color Centroid (Mean)		
	X	Y	Z	X	Y	Z
Expert						
E1	.247(*)	.197	.011	.160	.179	.028
E2	-.020	-.074	-.232(*)	-.040	-.017	-.174
E3	.256(*)	.160	-.051	.004	.034	-.111
Novice						
N1	-.159	-.135	-.188	.049	.058	.071
N2	.254(*)	.139	-.092	-.050	-.018	-.168
N3	.414(**)	.373(**)	.177	.334(**)	.364(**)	.246(*)

CIExyy’

	Color Variation (STD)			Color Centroid (Mean)		
	X	Y	Y’	X	Y	Y’
Expert						
E1	-.087	.276(*)	.197	.022	.389(**)	.179
E2	-.086	.212	-.074	.139	.350(**)	-.017
E3	-.044	.512(**)	.160	-.028	.480(**)	.034
Novice						
N1	.057	.091	-.135	-.038	.154	.058
N2	-.029	.621(**)	.139	.059	.471(**)	-.018
N3	.132	.350(**)	.373(**)	-.150	.417(**)	.364(**)

CIELab

	Color Variation (STD)			Color Centroid (Mean)		
	L	A	B	L	A	B
Expert						
E1	.363(**)	-.095	-.027	.159	-.209	.294(**)
E2	.251(*)	-.143	-.120	-.025	-.068	.311(**)
E3	.621(**)	-.246(*)	.126	-.003	-.360(**)	.393(**)
Novice						
N1	-.087	.214	-.138	.069	-.090	.091
N2	.663(**)	-.166	.086	-.057	-.299(**)	.397(**)
N3	.532(**)	.058	.257(*)	.341(**)	-.405(**)	.282(*)

CIELch

	Color Variation (STD)			Color Centroid (Mean)		
	L	C	H	L	C	H
Expert						
E1	.363(**)	-.123	-.267(*)	.159	-.043	.051
E2	.251(*)	-.217(*)	-.381(**)	-.025	.052	-.107
E3	.621(**)	-.070	-.343(**)	-.003	-.255(*)	-.120
Novice						
N1	-.087	.011	-.119	.069	-.025	.110
N2	.663(**)	-.094	-.271(*)	-.057	-.154	-.069
N3	.532(**)	.212	-.219(*)	.341(**)	-.232(*)	.001

CIELuv

	Color Variation (STD)			Color Centroid (Mean)		
	U	V	L	U	V	L
Expert						
E1	-.083	-.105	.202	-.106	.339(**)	.126
E2	-.092	-.148	-.068	.036	.358(**)	-.029
E3	-.195	.302(**)	.167	-.201	.473(**)	.026
Novice						
N1	.144	-.223(*)	-.135	-.089	.104	.062
N2	-.117	.226(*)	.144	-.107	.465(**)	-.029
N3	.084	.242(*)	.368(**)	-.290(**)	.321(**)	.395(**)

HSV

	Color Variation (STD)			Color Centroid (Mean)		
	H	S	V	H	S	V
Expert						
E1	.142	.401(**)	.414(**)	.023	.306(**)	.114
E2	.223(*)	.456(**)	.342(**)	.101	.107	-.067
E3	.037	.569(**)	.737(**)	-.068	.497(**)	-.096
Novice						
N1	-.102	-.025	-.117	-.033	-.013	.024
N2	.119	.588(**)	.786(**)	.074	.542(**)	-.156
N3	.031	.131	.510(**)	.038	.530(**)	.218(*)

HSL

	Color Variation (STD)			Color Centroid (Mean)		
	H	S	L	H	S	L
Expert						
E1	.142	.401(**)	.181	.023	.306(**)	-.100
E2	.223(*)	.456(**)	-.002	.101	.107	-.263(*)
E3	.037	.569(**)	.284(**)	-.068	.497(**)	-.193
Novice						
N1	-.102	-.025	-.051	-.033	-.013	.070
N2	.119	.588(**)	.258(*)	.074	.542(**)	-.234(*)
N3	.031	.131	.269(*)	.038	.530(**)	.225(*)

**. Correlation is significant at the 0.01 level (2-tailed).

*. Correlation is significant at the 0.05 level (2-tailed).

REFERENCES

[1] Abbasi, N. R., Shaw, H. M., Rigel, D. S., Friedman, R. J., McCarthy, W. H., Osman, I., Kopf, A.W., & Polsky, D. Early diagnosis of cutaneous melanoma: revisiting the ABCD. *The Journal of the American Medical Association, 292(22),* 2771-2776.2004.

[2] Abdel-Hakim, A. E.& Farag, A. A.(2005). Color Segmentation Using an Eigen Color Representation. *7th International Conference on Information Fusion, 2,* 1576 – 1583.

[3] Adam, M. B., & Reyna, V. F. (2005). Coherence and correspondence criteria for rationality: experts' estimation of risks of sexually transmitted infections. *Journal of Behavioral Decision Making, 18(3),* 169-186.

[4] Agarwal, S., Madasu, S., Hanmandlu, M., & Vasikarla, S. (2005). A comparison of some clustering techniques via color segmentation. *International Conference on Information Technology: Coding and Computing, 2,* 147 – 153.

[5] Aitken, J. F., Pfitzner, J., Battistutta, D., O'Rourke P. K., Green A. C., & Martin N. G. (1996). Reliability of computer image analysis of pigmented skin lesions of Australian adolescents. *Cancer, 78,* 252-257.

[6] Allen, J. T. & Huntsberger, T. (1989). Comparing color edge detection and segmentation methods. *IEEE Southeastcon '89. Proceedings of Energy and Information Technologies in the Southeast, 2,* 722 – 728.

[7] American Academy of Dermatology. (n.d.). Retrieved July 01, 2006, from http://www.aad.org/default.htm

[8] Bleakley, A., Farrow, R., & Gould, D. (2003). Learning how to see: Doctors making judgments in the visual domain. *Journal of Workplace Learning, 15(7-8), Special issue: Selected papers from the 3rd International Conference on Researching Work and Learning, Tampere, Finland: Part One,* 301-306.

[9] Bostock, R. T. J., Claridge, E., Harget, A. J., & Hall, P. N. (1993). Towards a neural network based system for skin cancer diagnosis. *Artificial Neural Networks, Third International Conference,* 215 – 219.

[10] Brainerd, C. J. & Reyna, V. F. (1990). Gist is the grist: Fuzzy-trace theory and the new intuitionism. Developmental Review, 10(1), Special issue: Limited resource models of cognitive development. 3-47.

[11] Carrara, M., Tomatis, S., Bono, A., Bartoli, C., Moglia, D., Lualdi, M. Colombo, A., Santinami, M., & Marchesini, R. (2005). Automated segmentation of pigmented skin lesions in multispectral imaging. *Physics in Medicine and Biology,* N345-N357.

[12] Casanova, D., Bardot, J., Aubert, J. P., Andrac, L., & Magalon, G. (1996). Management of nevus spilus. *Pediatric Dermatology, 13(3),* 233-238.

[13] Celebi, M. E., Aslandogan, Y. A. & Bergstresser, P. R. (2005). Mining biomedical images with density-based clustering. *International Conference on Information Technology: Coding and Computing, 1,* 163-168.

[14] Chang, Y., Stanley, R. J., Moss, R. H., & Van Stoecker, W. (2005). A

systematic heuristic approach for feature selection for melanoma discrimination using clinical images. *Skin Research and Technology, 11(3),* 165-78.

[15] Chen, H.-C., Chien, W.-J. & Wang, S.-J. (2002). Contrast based color Segmentation with adaptive thresholds. *Proceedings of International Conference on Image Processing, 2,* II-73 - II-76.

[16] Cheng, S.-C. (2003). Region-growing approach to colour segmentation using 3D labeling, clustering and relaxation. Proceedings of IEEE, Vision, Image and Signal Processing, 150 (4), 270 – 276.

[17] Coulter, J. S. (1991). ABCD's assessing skin lesions. *Advancing Clinical Care, 6(6),* 18-19.

[18] Cowan, J. M., Hablan, R., & Francke, U. (1988). Cytogenetic analysis of melanocytes from premalignant nevia and melanomas. *Journal of the National Cancer Institute, 80,* 1159-1164.

[19] Chung, D. H., & Sapiro, G. (2000). Segmenting skin lesions with partial-differential-equations-based image processing algorithms. *IEEE Transactions on Medical Imaging*, *19(7),* 763-767.

[20] Deng, Y., Kenney, C., Moore, M. S., & Manjunath, B. S. (1999). Peer group filtering and perceptual color image quantization. Proceedings of IEEE International Symposium on Circuits and Systems, 4, 21-24.

[21] De Weert, C. M. M. (1998). The use of color in visual displays. In G. C. van der Veer & G. Mulder (Eds.) *Human-computer interaction: psychonomic aspects.* New York: Springer-Verlag.

[22] Dhawan, A. P., Kini, P. & Sicsu, A. (1989). Imaging skin-lesions for detecting skin-cancer through image analysis. *Proceedings of the Annual International Conference of the IEEE Engineering in Engineering in Medicine and Biology Society, Images of the Twenty-First Century, 2,* 388 – 390.

[23] Donohoe, G. W., Nemeth, S., & Soliz, P.(1998). ART-based image analysis for pigmented lesions of the skin. *Proceedings of 11th IEEE Symposium on Computer-Based Medical Systems,* 293 - 298

[24] Dreiseitl, S., Ohno-Machado, L., Kittler, H., Vinterbo, S., Billharrt, H., & Binder, M. (2001). A comparison of machine learning methods for the diagnosis of pigmented skin lesions. *Journal of Biomedical Informatics, 34,* 28-36.

[25] Ekman, G. (1954). Dimensions of color vision, *The Journal of Psychology*, *38,* 467-474.

[26] Ercal, F., Chawla, A., Stoecker, W. V., Lee, H-C., & Moss, R. H. (1994). Neural network diagnosis of malignant melanoma from color images. *IEEE Transactions on Biomedical Engineering, 41(9),* 837 – 845.

[27] Fairhall, A. L., Burlingame, C. A., Narasimhan, R., Harris, R. A., Puchalla, J. L., & Berry, M. J. (2006). Selectivity for multiple stimulus features in retinal ganglion cells. *Journal of Neurophysiology, 96(5),* 2724-2738.

[28] Foley, J. D.,van Dam, A., Feiner, S. K. & Hughes, J. F. (1990). *Computer Graphics, Principles and Practice (2nd ed),* Addison-Wesley: New York.

[29] Fuh, C.-S., Cho, S. –W. & Essig, K. (2005). Hierarchical color image region

segmentation for content-based image retrieval system. *IEEE Transactions on Image Processing, 9(1),* 156 – 162.

[30] Gaines, R. (1975). Developmental perception and cognitive styles: from young children to master artists. *Perceptual and Motor Skills, 40(3),* 983-998.

[31] Ganster, H., Gelautz, M. Pinz, A. Binder, M., Pehamberger, H., Bammer, M., & Krocza, J. (1995). Initial results of automated melanoma recognition. *Theory and Applications of Image Analysis II, Selected papers of the 9th Scandinavian Conference Image Analysis*, *Singapore*, 343-354.

[32] Ganster, H., Pinz, P., Rohrer, R., Wildling, E., Binder, M., & and Kittler, H.(2001). Automated melanoma recognition, *IEEE Transactions on Medical Imaging*, *20(3),* 233-239.

[33] Garcia, C., & Tziritas, G. (1999). Face detection using quantized skin color regions merging and wavelet packet analysis. *IEEE Transactions on Multimedia, 1(3),* 264-277.

[34] Gauch, J.(1998). Segmentation and edge detection. In S. J. Sangwine & R. E. N. Home (Eds.), *The Colour Image Processing Handbook, pp.163-187.* Cambridge, Great Britain: Chapman & Hall.

[35] Gernsbacher, M. A. (1993). Less skilled readers have less efficient suppression mechanisms. *Psychological Science, 4(5),* 294-298.

[36] Gonzalez, C. R., & Woods, E. R. (1995). *Digital Image Processing.* Reading, MA: Addison-Wesley.

[37] Green, A., Martin, N., McKenzie, G., Pfitzner, J., Quintarelli, F., & Thomas, B.

W.(1991). Computer image analysis of pigmented skin lesions. *Melanoma Research, 1,* 231-236.

[38] Goldstein, B. G. & Goldstein, A. O. (2001). Diagnosis and Management of Malignant Melanoma, *American Family Physician, 63(7),* 1359-1368.

[39] Hall, P. N., Claridge, E., & Smith, J. D. M. (1995). Computer screening for early detection of melanoma—Is there a future? *British Journal of Dermatology, 132,* 325-338.

[40] Hashim, H., Ali, M. T., & Talib, N. A. (2005). Skin lesions color analysis based on RGB reflectance indices. Sensors and the International Conference on new Techniques in Pharmaceutical and Biomedical Research, Asian Conference, 94 – 98.

[41] Hashim, H., Jailani, R., & Taib, M. N. (2002). A visual record of medical skin disease imaging using MATLAB tools. Student Conference on Research and Development, 40-44.

[42] Health-Care.Net (n.d.). Retrieved September 01, 2006 from http://skin care.health-cares.net/skin-lesions.php

[43] Hurlbert, A. C. (1998). Computational models of color constancy. In Walsh, V. & Kulikowski, J. (Eds.), *Perceptual constancy: Why things look as they do,* pp. 283-322, New York, NY, US: Cambridge University Press.

[44] Itti, L., Koch, C., & Niebur, E. (1998). A model of saliency-based visual attention for rapid scene analysis. *IEEE Transactions on Pattern Analysis and Machine Intelligence, 20(11),* 254-1259.

[45] Jailani, R., Hashim, H., & Nasir Taib, M. (2005). Normalization techniques for

psoriasis skin lesion analysis. *Asian Conference on Sensors and the International Conference on new Techniques in Pharmaceutical and Biomedical Research,* 151 – 153.

[46] Josef, F. Melanocytic tumors, retrieved October 01, 2006 from http://atlases.muni.cz/atl_en/main+nadory+melantum.html#melnevus+melnevuscom

[47] Katz, R. C., & Jernigan, S., (1991). Brief report: An empirically derived educational program for detecting and preventing skin cancer. *Journal of Behavioral Medicine, 14(4),* 421-428.

[48] King, D. L. (2002). A brief delay decreases perceived similarity and improves discrimination. *Journal of General Psychology, 129(2),* 192-201.

[49] Kjoelen, A., Thompson, M., Umbaugh, S., Moss, R., & Stoecker, W. (1995). Performance of AI methods in detecting melanoma. *IEEE Engineering in Medicine and Biology, 14(4),* 411-416.

[50] Krauskopf, J. & Farell, B. (1991). Vernier acuity: effects of chromatic content, blur and contrast. *Vision research, 31(4),* 735-49.

[51] Lagarias, J. C., Reeds, J. A., Wright, M. H., & Wright, P. E. (1998). Convergence properties of the Nelder-Mead simplex method in low dimensions. *SIAM Journal of Optimization, 9 (1),* 112-147.

[52] Larkin, J., McDermott, J., Simon, D. P., & Simon, H. A. (1980). Expert and novice performance in solving Physics problems, *Science, 208,* 1335-1342.

[53] Lee, T., Ng, V., McLean, D., Coldman, A., Gallagher, R., & Sale, J. (1995). A

multi-stage segmentation method for images of skin lesions. *Proceedings of IEEE Pacific Rim Conference on Communications, Computers, and Signal Processing,* 602 – 605.

[54] Lee, T., Ng, V., Gallagher, R., Coldman, A. & McLean, D.(1997). DullRazor: a software approach to hair removal from images. *Computers in Biology and Medicine*, *27,* 533-543.

[55] Maglogiannis, I., Caroni, C., Pavlopoulos, S., Karioti, V., & Koutsouris, D. (2001). Utilizing artificial intelligence for the characterization of dermatological images. *Proceedings of 4th International Conference Neural Networks and Expert Systems in Medicine and Healthcare,* 362-368.

[56] Maglogiannis, I., & Kosmopoulos, D. (2003). A digital image acquisition system for skin lesionsin. *SPIE International Conference Medical Imaging, San Diego, CA,* 15–20.

[57] Maglogiannis, I., Pavlopoulos, S., & Koutsouris, D. (2005). An integrated computer supported acquisition, handling, and characterization system for pigmented skin lesions in dermatological images. *IEEE Transactions on Information Technology in Biomedicine, 9(1),* 86-98.

[58] Mardia, K. V., Kent, J. T., & Bibby, J. M. (1979). *Multivariate Analysis* London. U.K.: London Academic Press.

[59] Mickler, T. J., Rodrigue, J. R., & Lescano, C., M. (1999). A comparison of three methods of teaching skin self-examinations*, Journal of Clinical Psychology in Medical Settings, 6(3),* 273-286.

[60] Mikkilineni, R., Weinstock, M.A., Goldstein, M. G., Dube, C. E., & Rossi, J. S.(2002). The impact of the basic skin cancer triage curriculum on providers' skills, confidence, and knowledge in skin cancer control. *Preventive Medicine: An International Journal Devoted to Practice & Theory, 34(2),* 144-152.

[61] Moghaddamzadeh, A. & Mohsenian, N. (1996). An object-based approach to color subsampling. *IEEE International Conference on Conference Proceedings of Acoustics, Speech, and Signal Processing, 4,* 1894 – 1897.

[62] Mojsilovic, A., Hu, H. & Soljanin, E. (2002). Extraction of perceptually important colors and similarity. *IEEE Transactions on Image Processing of Measurement for Image Matching, Retrieval and Analysis, 11,* 1238-1248.

[63] Muglia, J. J., Pesce, K., & McDonald, C. J. (1999). Skin cancer screening: A growing neeed, *Surgical Oncology Clinics of North America, 8(4),* 735-745.

[64] Murphy, G. F., Kwan, T. H., & Mihm, M. C.(1984). The skin. In: S.L. Robbins, R. S. Cotran, & V. Kumar (Eds.), *Pathologic Basis of Disease.* (3rd ed., pp. 1257-1304). Philadelphia, PA :W.B. Saunders.

[65] Müller, H. J. & Krummenacher, J. (2006). Visual search and selective attention. *Visual Cognition, 14(4-8), Special issue: Visual search and attention,* 389-410.

[66] Nachbar, F., Stolz, W., Merkle, T., Cognetta, A. B., Vogt, T. & Landthaler, M. et al. (1994). The ABCD rule of dermatoscopy: high prospective value in the diagnosis of doubtful melanocytic skin lesions. *Journal of American Academy of Dermatology*, *30(4),* 551-559.

[67] Neviata R. (1977). A color edge detection and its use in scene segmentation.

IEEE Transactions on System, Man, Cybernet, SMC-7, 820–826.

[68] Ng, V., Cheung, D., & Fu, A. (1995). Medical image retrieval by color content. *IEEE International Conference on Systems, Man and Cybernetics, Intelligent Systems for the 21st Century, Vancouver, Canada, 3,* 1980 – 1985.

[69] Pariser, R. J. (1998). Benign neoplasms of the skin. *Medical Clinics of North America, 82,* 1285-1307.

[70] Pariser R. J., & Pariser, D. M. (1987). Primary care physicians errors in handling cutaneous disorders. *Journal of American Academy of Dermatology, 17,* 239-245.

[71] Peddie, W. (1940). Colour vision and chromaticity scales. *Nature, 146,* 717-718.

[72] Pompl, R., Bunk, W., Horsch, A., Abmayr, W., Morfill, G., Brauer, W., & Stolz, W. (1999). Computer vision of melanocytic lesions using MELDOQ, *Proceedings of 6th Congress International Society Skin Imaging, London, U.K., 5(2),* 150.

[73] Popkin, G. L. (1990). Tumors of the skin: a dermatologist's viewpoint. In: J. G. McCarthy (ed.) *Plastic Surgery, 5,* pp. 3560-3613.

[74] Ouyang A., & Tan, Y. –P.(2002). A novel multi-scale spatial-color descriptor for content-based image retrieval. *7th International Conference on Control, Automation, Robotics and Vision, 3,* 1204 – 1209.

[75] Roning, J., & Riech, M. (1998). Registration of nevi in successive skin images for early detection of melanoma. *Proceedings of Fourteenth International Conference on Pattern Recognition, Australia,* 1, 352-357.

[76] Round, A. J., Duller, A.W.G., & Fish, P. J. (1997). Colour segmentation for

lesion classification. *Proceedings of the 19th Annual International Conference of the IEEE Engineering in Medicine and Biology society, 2(30),* 582 – 585.

[77] Rosai, J. (1989). The skin: dermatoses and tumorlike conditions. *Ackerman's Surgical Pathology, 1,* 153-172.

[78] Ross, T., Handels, H., Kreusch, J., Busche, H., Wolf, H. H., & Pöppl S.T. (1995). Automatic classification of skin tumours with high resolution surface profiles. *Proceedings of Computer Analysis of Images and Patterns, Berlin, Germany,* 368-375.

[79] Scheunders, P. (1996). A genetic approach towards optimal color image quantization. *Proceedings of International Conference on Image Processing, 3,* 1031 – 1034.

[80] Schmid, P. (1999). Segmentation of digitized dermatoscopic images by two dimensional color clustering. *IEEE Transactions on Medical Imaging, 18(2),* 164-171.

[81] Schmid, P. & Fischer, S. (1997). Colour segmentation for the analysis of pigmented skin lesions. *Sixth International Conference on Image Processing and Its Applications, 2,* 688 – 692.

[82] Schneider, N., & von Campenhausen, C. (1998). Color and lightness constancy in different perceptual tasks. *Biological Cybernetics, 79(6),* 445-55.

[83] Schindewolf, T., Schiffner, R., Stoltz, W., Albert, R., Abmayr, W., & Harms, H. (1994). Evaluation of different image acquisition techniques for a computer vision system in the diagnosis of malignant melanoma. *Journal of American Academy of Dermatology, 31(1)*, 33-41.

[84] Shackelford, A. K., & Davis, C. H. (2003).A combined fuzzy pixel-based and

object-based approach for classification of high-resolution multispectral data over urban areas. *IEEE Transactions on Geoscience and Remote Sensing, 41(10),* 2354 – 2363.

[85] Silver, S. G., & Ho, V. C. (2003). Benign epithelial tumors. In T. B. Fitzpatrick, I .M. Freedberg, & A. Z. Eisen, et. al (Eds), *Dermatology in General Medicine,* (6th ed., pp. 767-785). New York: McGraw-Hill.

[86] Sirisathitkul, Y., Auwatanamongkol, S., & Uyyanonvara, B. (2004). Fast color image quantization using squared Euclidean distance of adjacent color points along the highest color variance axis. *Proceedings of the 17th International Conference on Pattern Recognition, 1,* 656-659.

[87] Tversky, A., & Kahneman, D., (1974). Judgment under uncertainty: Heuristics and biases, *Science, 185,* 1124-1131.

[88] The MathWorks. (n.d.). Color Space Conversion. Retrieved September 01, 2006, from http://www.mathworks.com/access/helpdesk/help/toolbox/vipblks/colorspaceconversion.html

[89] Tseng, D.-C. & Chang, C.-H. (1992). Color segmentation using perceptual attributes. Proceedings of 11th International Conference on Pattern Recognition, Conference C: Image, Speech and Signal Analysis, 3, 228 – 231.

[90] Umbaugh, S. E., Moss, R.H., & Stoecker, W.V. (1991). Applying artificial intelligence to the identification of variegated coloring in skin tumors. *Engineering in Medicine and Biology Magazine, IEEE, 10(4),* 57 – 62.

[91] Umbaugh, S. E., Moss, R. H., Stoecker, W. V., & Hance, G. A. (1993).

Automatic color segmentation algorithms-with application to skin tumor feature identification. *Engineering in Medicine and Biology Magazine, IEEE, 12(3),* 75-82.

[92] Vannoorenberghe, P., Colot, O., & de Brucq, D. (1999). Dempster-Shafer's theory as an aid to color information processing application to melanoma detection in dermatology. *Proceedings of the 10th International Conference on Image Analysis and Processing,* 774.

[93] Venot, A., Devaux, J., Herbin, M. Lebruchec, J. Dubertret, L., Raulo, Y., & Roucayrol, J. (1988). An automated system for the registration and comparison of photographic images in medicine. *IEEE Transactions on Medical Imaging, 7(4),* 298-303.

[94] Wandell, B. A. (1993). Color Appearance: the Effects of Illumination and Spatial Patterns. *Proceedings of the National Academy of Sciences of the United States of America, 90,* 1494-1501.

[95] Weiss, S. M., & Kulikowski, C. A. (1991). *Computer Systems That Learn: Classification and Prediction Methods from Statistics, Neural Nets, Machine Learning and Expert Systems.* San Mateo, CA: Morgan Kaufmann.

[96] Wikipedia, CIE 1931 color space. (n.d.). Retrieved July 1, 2006, from http://en.wikipedia.org/wiki/CIE_1931_color_space

[97] Wolfe, J. M., Butcher, S. J., & Lee, C. (2003). Changing your mind: On the contributions of top-down and bottom-up guidance in visual search for feature singletons. *Journal of Experimental Psychology: Human Perception and Performance, 29(2),* 483-502.

[98] Xu, L., Jackowski, M., Goshtasby, A., Roseman, D., Bines, S., Yu, C., Dhawan, A., & Huntley, A. (1999). Segmentation of skin cancer images. *Image Vision Comput., 17,* 65-74.

[99] Yamagishi, N. (1996). Roles of chromatic and luminance information in pattern recognition. *Dissertation Abstracts International: Section B: The Sciences & Engineering, 57,* 2193.

[100] Yoon, K-J., & Kweon, I-S., (2004). Human perception based color image quantization. *Proceedings of the 17th International Conference on Pattern Recognition, 1,* 664-667.

[101] Zagrouba, E., & Barhoumi, W. (2003). Objective and cost-efficient approach for skin lesions classification. *ACS/IEEE International Conference on Computer Systems and Applications, Book of Abstracts,* 135.

[102] Zarem H. A. & Lowe N. J. (1997). Benign growths and generalized skin disorders. In S. J. Aston, R. W. Beasley, & C. H. Thorne(Eds.) *Grabb and Smith's Plastic Surgery*. (5th ed., p. 148). Philadelphia: Lippincott-Raven.

[103] Zaqout, I., Zainuddin, R., & Baba, S. (2005). Pixel-based skin color detection technique. Machine Graphics & Vision International Journal, 14(1). 61 – 70.

[104] Zhang, J., Change, C. I., Miller, S. J., & Kang, K. A. (2000). A feasibility study of multispectral image analysis of skin tumors. *Biomedical Instrumentation and Technology, 34(4),* 275-282.

[105] Zhishun, S., Fish, P. J. & Duller, A. W. G. (2001). Simulation of optical skin

lesion images. Proceedings of the 23rd Annual International Conference of the IEEE: Engineering in Medicine and Biology Society, 3, 2766 – 2769.

[106] Zhong, D.X., & Yan, H. (2000). Color image segmentation using color space analysis and fuzzy clustering. *Proceedings of the 2000 IEEE Signal Processing Society Workshop Neural Networks for Signal Processing, 2,* 624 – 633.

BIOGRAPHICAL INFORMATION

Yu-Chin Chai received a Ph.D. degree in Experimental Psychology with a concentration in attention and complexity from the University of Texas at Arlington in August, 2004. She earned a Bachelor of Science Degree in psychology from National Cheng-Chi University, Taiwan, June 1996. She had received a research scholarship from Taiwan National Science Council in 1995. She started her research with Dr. Brown in a direction of attention and negative priming from fall, 1996 to fall, 1997. Later, she worked with Dr. Hillstrom from summer, 2000 to 2004. She earned a Master of Science degree in experimental psychology with a concentration in object recognition and perception from the University of Texas at Arlington, May 2003. She earned a Master of Science Degree in Computer Science and Engineering on the topic related to the pigmented skin lesion study and with a major track in database. She is currently working as post-doctoral fellow in Institute of Sensory Research, Department of Biomedical and Chemical Engineering, Syracuse University.